

Neutral triplet collective mode as a decay channel in graphite

M. Ebrahimkhas¹ and S. A. Jafari^{2,*}¹Department of Science, Tarbiat Modarres University, Tehran 14115–175²Department of Physics, Isfahan University of Technology, Isfahan 84156-83111, Iran

(Received 7 February 2009; published 22 May 2009)

In an earlier work we predicted the existence of a neutral triplet collective mode in undoped graphene and graphite [G. Baskaran and S. A. Jafari, Phys. Rev. Lett. **89**, 016402 (2002)]. In this work we study a phenomenological Hamiltonian describing the interaction of tight-binding electrons on honeycomb lattice with such a dispersive neutral triplet boson. Our Hamiltonian is a generalization of the Holstein polaron problem to the case of triplet bosons with nontrivial dispersion all over the Brillouin zone. This collective mode constitutes an important excitation branch which can contribute to the decay rate of the electronic excitations. The presence of such collective mode modifies the spectral properties of electrons in graphite and undoped graphene. In particular such collective mode, as will be shown in this paper, can account for some parts of the missing decay rate in a time-domain measurement of the excitation lifetime in graphite.

DOI: 10.1103/PhysRevB.79.205425

PACS number(s): 72.15.Nj, 72.10.Di

I. INTRODUCTION

Recently Novoselov *et al.*¹ was able to fabricate graphene, a single atomic layer of graphite. This discovery has brought graphene to the center of attention of many researchers.² The fundamental difference of the electronic spectrum of graphene with respect to the usual metals is the existence of Fermi points around which an effective Dirac theory describes the electronic states.³ The suspended graphene can now be fabricated in which the effects of impurity and substrate are substantially reduced and one can approach the ballistic limit of transport with Dirac electrons.⁴

Starting from a single layer of graphene, and adding further layers, one obtains graphene multilayers. For few layers the even-odd effects due to quantum confinement arise.² However, as the number of layers exceeds ~ 10 , one approaches the bulk limit, or graphite. The Dirac part of the energy dispersion of graphite is qualitatively similar to graphene.⁵ The only important difference between the electronic states of graphite and graphene is the presence of small pockets up to ~ 40 meV, beyond which the Dirac description applies to the low-energy physics of graphite as well.^{6,7} Ignoring such pockets which originate from the weak interlayer coupling, the electronic structure of bulk graphite can be approximately described by a tight-binding model on a two-dimensional (2D) honeycomb lattice. In our approach both highly oriented pyrolytic graphite (HOPG) and undoped graphene are treated within this model. The calculations of this paper are aimed to explain the lifetime anomaly in HOPG but apply to undoped graphene as well.

The presence of Dirac points makes the nature of particle-hole excitations in graphene drastically different from the system possessing extended Fermi surface. Due to such conelike spectrum, there will be a region below the particle-hole continuum, where no particle-hole pairs can exist. Such a “window” does not exist in usual metals.⁸ A simple random-phase-approximation (RPA) analysis shows that the presence of such window below the particle-hole continuum provides a unique opportunity for the existence of a triplet bound state of electron-hole excitation.⁸ An intuitive way to

understand such a triplet electron-hole bound state is to view the semimetallic graphene from the semiconducting side. From this point of view, such collective excitation can be regarded as the analog of triplet excitons.⁹

In this work we focus on the time-domain lifetime measurements performed on HOPG samples which correspond to the *undoped* graphite. The time resolved photoemission spectroscopy (TRPES) made by Moos *et al.*¹⁰ on HOPG was employed to measure the decay rate of quasiparticles (QPs) in graphite. There are two salient features of the TRPES experiment reported by Moos *et al.*¹⁰ which for convenience has been included in Fig. 1. (i) The plateau in the energy range 1–2 eV is already a marked deviation from the Fermi-liquid prediction which was qualitatively explained in Refs. 10 and 11, in terms of the peculiar form of the graphite dispersion near the saddle point. Such a plateau has been reported in the carrier lifetime of doped graphene in angular resolved photoemission spectroscopy (ARPES) experiments as well¹² which can be understood in terms of a similar G_0W type of treatment.¹³ The presence of plateau can be justified in terms of kinematic constraints for the decay of quasiparticles from the M point.¹⁰ (ii) The second important observation of the above TRPES experiment was that the decay rate of excitations in the whole range of energies over which the measurement was performed was larger than the *ab initio* calculation of Ref. 11. This clearly means that there should be another decay channel for quasiparticles, especially in the energy range 1–2 eV. In the whole measurement range the experimentally observed decay rate is almost a factor of 2 larger than the GW calculation.

Obviously the phonons cease to exist beyond 0.2 eV, and hence cannot be responsible for the missing decay channel in the energies reported in Ref. 10. Moreover, both in HOPG and undoped graphene, there are no plasmons whatsoever.^{14,15} Therefore we believe that this lifetime experiment already points to the existence of an unnoticed bosonic branch of neutral excitations.^{8,9} There are also other evidences based on the Fermi velocity renormalization measurements. If one appeals to electron-phonon coupling to explain the experimentally observed reduction in the Fermi velocity v_F with respect to the band-structure prediction, one

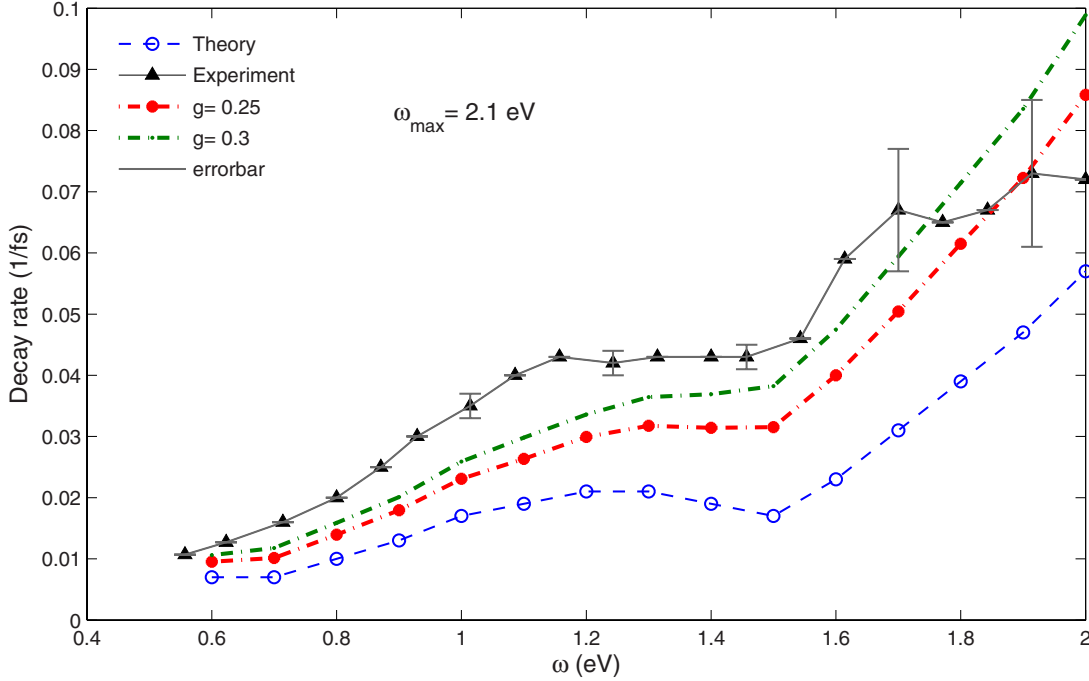


FIG. 1. (Color online) Quasiparticle decay rate in HOPG graphite. The triangles indicate TRPES measurements in Ref. 10, the open circles are the *ab initio* GW calculation of Ref. 11. Filled circles and dashed lines show the total decay rate in the presence of a new decay mechanism caused by triplet bosons for the electron-boson couplings $g=0.25, 0.3$. In this calculation we have taken $\omega_{\max}=2.1$ eV. See the text for explanation.

has to use an electron-phonon coupling which is almost ~ 5 times larger than the density-functional theory estimates.¹⁶ Therefore it seems that the phonons are not enough to account for about 20% Fermi velocity renormalization.¹⁶ The second experimental hint for the existence of such a bosonic mode is the remarkable observation of the Bose metal-insulator transition tuned by magnetic field¹⁷ in graphite¹⁸ and graphene.¹⁹

Based on the above evidences, in this paper we employ a triplet bosonic mode predicted in Ref. 8 with a gapless dispersion of up to $\omega_{\max} \sim 2.1$ eV. Our model is a natural generalization of the polaron problem, with spin-flip processes included. We generalize the momentum average (MA) approximation developed in the context of the polaron problem by Berciu²⁰ to take into account the spin-flip vertices as well as the nontrivial dispersion in the spectrum of bosons. First we introduce our model and the MA method. Next we apply the MA approximation to discuss the coupling of a triplet boson to electronic states of graphene quasiparticles. The details of generalization of MA approximation to spin-flip processes are discussed in the Appendix.

II. MODEL AND METHOD

We start with Hamiltonian (1) describing the tight-binding electrons on the honeycomb lattice (first term), along with dispersive triplet bosons (second term) and the interaction between electrons and bosons (third term),

$$H = \sum_{\vec{k}, \alpha=\uparrow, \downarrow} \epsilon_{\vec{k}} c_{\vec{k}, \alpha}^{\dagger} c_{\vec{k}, \alpha} + \sum_{\vec{q}, m=\pm 1} \omega_{\vec{q}} S_{\vec{q}, m}^{\dagger} S_{\vec{q}, m} + g \sum_{\vec{k}, \vec{q}, m, m', \alpha, \alpha'} (S_{\vec{q}, m}^{\dagger} + S_{-\vec{q}, m'}) c_{\vec{k}-\vec{q}, \alpha}^{\dagger} c_{\vec{k}, \alpha'}, \quad (1)$$

where $\epsilon_{\vec{k}} = \pm t \sqrt{1 + \cos(\sqrt{3}k_y/2) \cos(k_x/2) + 4 \cos^2(k_x/2)}$ is the spectrum of fermions for (conduction or valence) band and $\omega_{\vec{q}}$ describes the dispersion of spin-1 bosons.⁸ Here $c_{\vec{k}, \alpha}^{\dagger}$ ($c_{\vec{k}, \alpha}$) is the creation (annihilation) operator for fermions with momentum \vec{k} and spin $\alpha = \uparrow, \downarrow$ in either of the valence or conduction bands, while $S_{\vec{q}, m}^{\dagger}, S_{\vec{q}, m}$ are the ladder operator for spin-1 bosons with momentum \vec{q} and magnetic quantum numbers $m = \pm 1, 0$. In this Hamiltonian, g is the coupling strength and describes how strongly the exchange of triplet excitons takes place among the electrons. Estimates of a similar coupling in doped solid C₆₀ suggests $g \sim 0.3$ for those systems.²¹ The presence of such term favors singlet pairing under suitable conditions.^{21,22}

The interaction term of Hamiltonian (1) describes both spin-flip ($m = \pm 1$) as well as non-spin-flip ($m = 0$) processes. Since non-spin-flip processes can exist in presence of spin-0 bosons as well, to isolate the contribution of the spin-flip processes, we focus on $m = \pm 1$ terms only. In this sector, requiring Hamiltonian (1) to be Hermitian gives rise to the following restrictions on the possible values of m, m', α, α' :

$$m = 1(-1) \rightarrow m' = -1(1) \rightarrow \alpha = \downarrow(\uparrow) \rightarrow \alpha' = \uparrow(\downarrow).$$

We use MA approximation to calculate the Green's function and self-energy of the system^{20,23} which yields various

physical quantities such as the decay rate. Comparison of MA and its descendants [e.g., MA(1), MA(2), etc.] with other methods demonstrated that this method is accurate for the entire spectrum (both low and high energy) and for all coupling strengths and in all dimensions.²³ This approximation was also used successfully for the analysis of the effects of ripples on the graphene sheet.²⁴ In the following, we use the MA(1) approximation, the details of which for the case of dispersive mode with spin-1 are derived in the Appendix.

The single electron Green's function can be written as

$$G_{\alpha,\beta}(\vec{k}, \tau) = -i\theta(\tau)\langle 0|c_{\vec{k},\alpha}e^{iH\tau}c_{\vec{k},\tau}^\dagger|0\rangle, \quad (2)$$

where α, β are the spin indices and $|0\rangle$ is the vacuum state. In the absence of bosons the free propagator is

$$G_0(\vec{k}, \omega) = \frac{1}{\omega - \epsilon_{\vec{k}} + i\eta}. \quad (3)$$

To take into account the coupling to triplet bosons, we use the equation of motion for $G_{\alpha,\beta}(\vec{k}, \tau)$ to obtain (see the Appendix)

$$G_{\alpha,\beta}(\vec{k}, \omega) = G_0(\vec{k}, \omega) \left[\delta_{\alpha,\beta} + g \sum_{\vec{q}_1, m_1} F_1^{\alpha,-\beta}(\vec{k}, \vec{q}_1, m_1; \omega) \right], \quad (4)$$

where

$$\Sigma^{\alpha,\alpha}(\omega) = \frac{g^2 \sum_{\vec{k}, \vec{q}_1} G_0[\vec{k} - \vec{q}_1, \omega - \omega_{\vec{q}_1} - g^2 A_1(\omega)]}{1 - g^2 \sum_{\vec{k}, \vec{q}_1} G_0[\vec{k} - \vec{q}_1, \omega - \omega_{\vec{q}_1} - g^2 A_1(\omega)] [A_2(\omega) - A_1(\omega)]}, \quad (8)$$

where A_1, A_2 are the functions of ω , defined in the Appendix. The self-energy contains all interaction effects and can be used to calculate spectral weights, decay rates, etc. in a straightforward way.²⁵

III. RESULTS

Now we are in the position to derive the decay rate or lifetime of QPs of HOPG or graphene in the presence of spin-1 bosonic collective mode. There are some other decay mechanisms such as electron-hole,¹¹ electron-phonon,²⁶ and electron-plasmon scatterings.¹⁴ In doped graphene, all the above mechanisms might contribute to the renormalization of QP properties. However, in HOPG graphite and undoped graphene there are no plasmons to couple to the electronic degrees of freedom.

A. Decay rate

The imaginary part of self-energy related to the lifetime and decay rate of QP,

$$F_1^{\alpha,-\beta}(\vec{k}, \vec{q}_1, m_1; \omega) = \langle 0|c_{\vec{k},\alpha} \frac{1}{\omega - \hat{H} + i\eta} c_{\vec{k}-\vec{q}_1,-\beta}^\dagger S_{\vec{q}_1, m_1}^\dagger |0\rangle. \quad (5)$$

Here, F_1 is the amplitude for the process in which the initial state contains a fermion and a boson, and the final states contain only a fermion with *opposite* spin. Hence, physically it corresponds to the amplitude of annihilating one triplet ($\Delta m = \pm 1$) boson. Applying again the equation of motion to F_1 generates hierarchy of equations containing amplitudes with multiboson states,

$$F_1^{\alpha,-\beta}(\vec{k}, \vec{q}_1, m_1, \omega) = G_0(\vec{k} - \vec{q}_1, \omega - \omega_{\vec{q}_1}) \left[g^2 + \sum_{\vec{q}_2, m_2} F_2^{\alpha,\beta}(\vec{k}, \vec{q}_1, \vec{q}_2, m_1, m_2; \omega) \right]. \quad (6)$$

Although each internal vertex may contain spin-flip scatterings, since Hamiltonian (1) preserves the spin, the incoming and outgoing fermions must have the same spin. Hence the Green's function (2) must be diagonal with respect to the spin indices. The rigorous proof of this is given in the Appendix. Also, by the Dyson equation, the self-energy is also diagonal with respect to spin indices,

$$G_{\alpha,\alpha}(\vec{k}, \omega) = [\omega - \epsilon_{\vec{k}} - \Sigma^{\alpha,\alpha}(\vec{k}, \omega) + i\eta]^{-1}. \quad (7)$$

The self-energy $\Sigma^{\alpha,\alpha}(\vec{k}, \omega)$ in the MA(1) approximation is given by (see the Appendix)

$$\frac{1}{\tau} \propto -\text{Im}[\text{Tr}\Sigma^{\alpha,\alpha}(\vec{k}, \omega)]. \quad (9)$$

We have numerically evaluated the integrals necessary to get self-energy (8). In Fig. 1, we have plotted the decay rate measured in the TRPES experiment of Ref. 10 (triangles) along with the electron-hole decay mechanisms captured within the GW approximation (open circles).¹¹ As can be seen in this figure, the decay into *incoherent* electron-hole pairs within the GW approximation can only account for half of the experimentally reported QP decay rate. In this figure, we plot the total decay rate in the presence of the spin-flip scatterings from a tripled bosonic mode for the coupling values $g=0.25$ (filled circles) and $g=0.3$ (dashed line). The triplet bosonic collective mode has a wide dispersion between zero and $\omega_{\text{max}} \sim 2.1$ eV.

As can be seen, a dispersive bosonic collective mode can account for the missing decay rate in HOPG graphite. The same result applies to undoped graphene as well. The fact that the GW approximation falls a factor of 2 behind the experimentally measured decay rate indicates that in addition

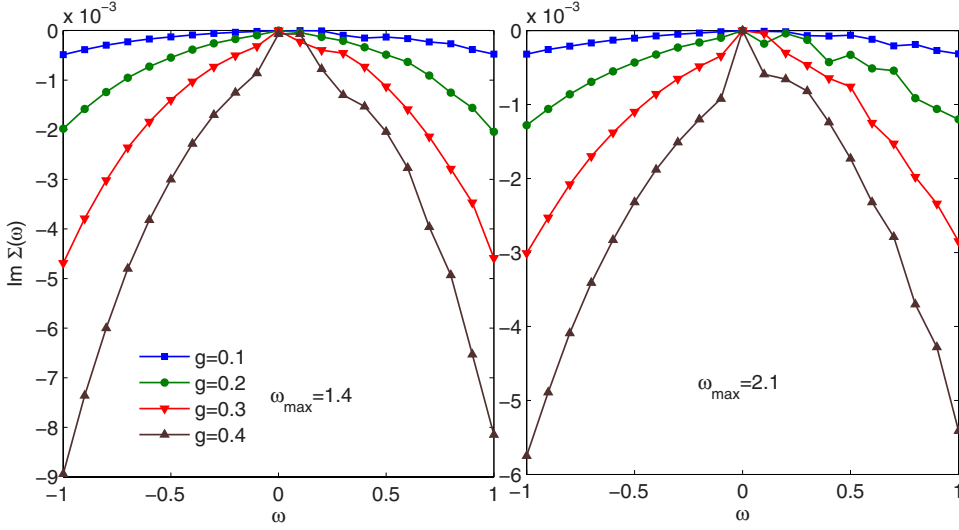


FIG. 2. (Color online) Imaginary part of self-energy vs energy (eV) for $\omega(q)_{\text{max}}=1.4$ eV and $\omega(q)_{\text{max}}=2.1$ eV.

to incoherent electron-hole decay processes, there should be another decay channel provided by a *coherent* bound state of electron-hole pairs, which is what our phenomenological Hamiltonian (1) describes. A simple RPA analysis showed that such a bound state can occur in the triplet channel.^{8,9}

B. Dependence on ω_{max}

The dispersion of the triplet bosonic mode is over a wide energy range from zero to $\omega_{\text{max}} \sim 2.1$ eV. The shape of the dispersion and the value of ω_{max} in the original work or Refs. 8 and 9 are essentially controlled by the short-range part of the interaction (Hubbard U). It was also shown that the long-range part of the Coulomb interaction does not play a crucial role in the dispersion of the spin-1 collective mode.⁹ In the

present calculation, we have fitted the dispersion relation obtained from the RPA analysis of Refs. 8 and 9 with ~ 10 cosine harmonics over the whole Brillouin zone.

In Fig. 2 we explore the dependence of decay rates on the dispersion bandwidth (ω_{max}). Left panel shows the imaginary part of the self-energy for various values of the electron-boson coupling g and for $\omega_{\text{max}}=1.4$, while the right panel shows the same result for $\omega_{\text{max}}=2.1$. As can be seen in both panels, by increasing the coupling strength g , the decay rate at a given energy scale increases. Comparison of the left and right panels for the same values of g shows that with a smaller width of dispersion (ω_{max}), the bosonic mode leads to stronger spin-flip scattering. The limit $\omega_{\text{max}} \rightarrow 0$ can be thought of as an Einstein-type phonon mode which was studied within MA(1) in Ref. 24. Smaller ω_{max} in our phenom-

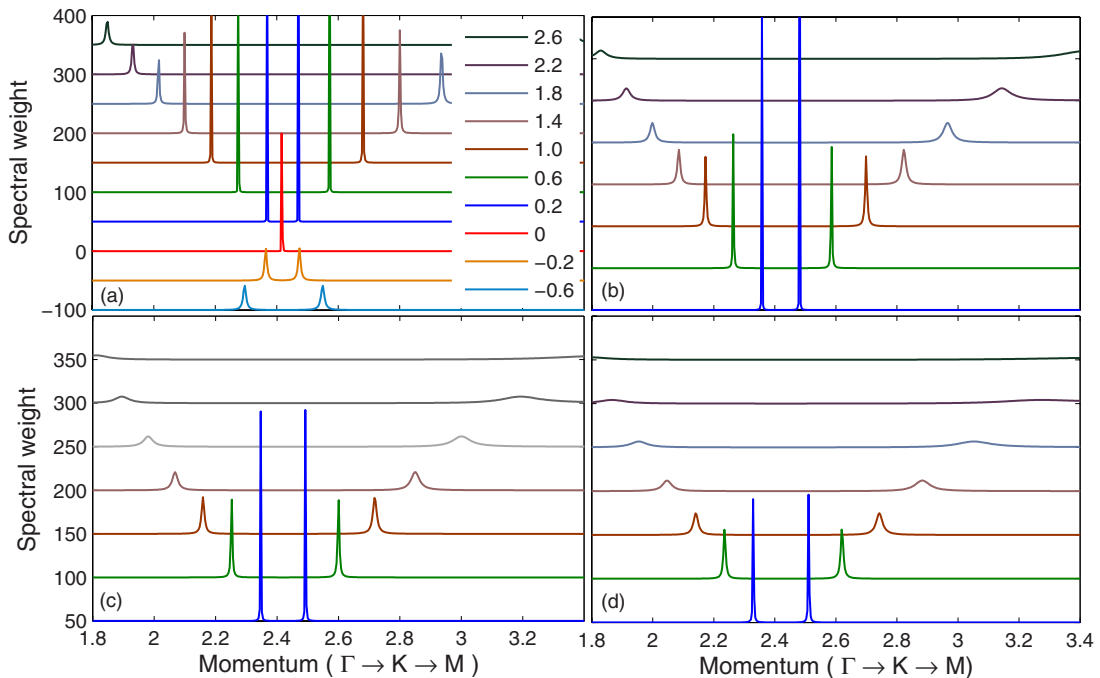


FIG. 3. (Color online) The spectral weight along the high-symmetry cut in the BZ for $\omega_{\text{max}}=2.1$ eV and (a) $g=0.3$ for different energy from -0.6 to 2.6 eV, (b) $g=0.6$, (c) $g=0.8$, and (d) $g=1.0$ for different energies from 0.2 to 2.6 eV

enological Hamiltonian (1) corresponds to larger U in the Hamiltonian of the original electrons in Ref. 9. Hence the observation of Fig. 2 can be justified as follows. In terms of the Hubbard-type Hamiltonian of Ref. 8, larger U naturally leads to stronger decay rates.

C. Spectral function

Once we calculate the self-energy $\Sigma^{\alpha,\alpha}(\omega)$ at any approximation, we are able to immediately calculate the spectral weight $A(\vec{k}, \omega) = -\frac{1}{2\pi} \text{Im}[\text{Tr} G_{\alpha,\alpha}(\vec{k}, \omega)]$. We have plotted the spectral weight along the high-symmetry cut Γ - K - M of the Brillouin zone in Fig. 3. We have plotted the spectral weight for different energies. Panels (a)–(d) correspond to different values of g as indicated in the figure caption.

The first point to notice in all panels is that the conelike dispersion of the Dirac electrons remains quite robust against the increase in the electron-boson coupling g . To see this more transparently, in panel (a) we have plotted some negative-energy spectral functions as well. As can be seen in panel (d), large values of coupling $g \sim 1$ lead to a remarkable broadening in the quasiparticle peaks. Direct comparison with ARPES experiments on graphene indicates that g cannot be as large as $g \sim 1$.

Negative-energy plots of panel (a) indicates that there is an asymmetry between the positive-energy states and the negative-energy states. This is natural, as the collective mode is an excitation and does not carry negative energies.

IV. CONCLUSION

In this work we considered a phenomenological Hamiltonian containing a neutral spin-1 collective mode as a different bosonic branch of excitations predicted to exist in HOPG and undoped graphene.⁸ Employing the momentum average self-energy we showed that such a coherent particle-hole bound state in the triplet channel can account for a substantial part of the missing decay rate in TRPES experiment of Ref. 10 in HOPG. Another supporting evidence for the existence of such a spin-1 collective mode which is a natural generalization of triplet excitations of ordinary semiconductors to the case of semimetallic HOPG comes from the downward renormalization of v_F .¹⁶ Apparently phonons fail to account for such renormalization. Moreover, the remarkable observation of Bose metal-insulator transition tuned by the magnetic field¹⁷ in HOPG (Ref. 18) and graphene¹⁹ might indicate that there such a spin excitation branch can have interesting consequences for the behavior of HOPG and graphene in magnetic fields.

ACKNOWLEDGMENTS

We wish to thank M. R. Abolhassani, Y. Kopelevich, M. Berciu, and G. Baskaran for comments and suggestions. S.A.J. was supported by the Vice Chancellor for Research Affairs of the Isfahan University of Technology and the National Elite Foundation (NEF) of Iran.

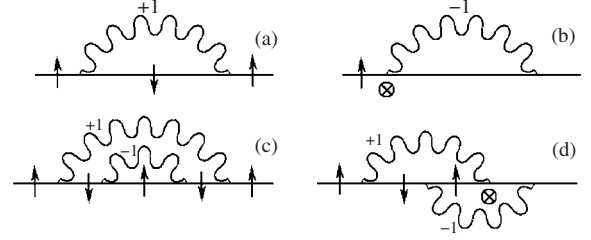


FIG. 4. First- and second-order Feynman diagrams for the scattering vertex from a spin-1 collective mode. At each vertex the spin of electron is flipped. Therefore, the incoming and outgoing spins end up to be identical as in diagrams (a) and (c). However, if we insist to have the spin of outgoing state to be opposite to that of incoming state, some vertices (denoted by \otimes) will not do flip the spin; that is they will not correspond to scattering from a spin-1 collective mode, as in diagrams (b) and (d).

APPENDIX: GENERALIZATION OF MA(1) FOR SPIN-FLIP HAMILTONIANS

We start by writing Eq. (4) with explicit spin indices. The matrix elements of the Green's function become

$$G_{\uparrow,\uparrow}(\vec{k}, \omega) = G_0(\vec{k}, \omega) \left[1 + g \sum_{\vec{k}, \vec{q}_1} F_1^{\uparrow,\uparrow}(\vec{k}, \vec{q}_1, +1; \omega) \right], \quad (\text{A1})$$

$$G_{\downarrow,\downarrow}(\vec{k}, \omega) = G_0(\vec{k}, \omega) \left[1 + g \sum_{\vec{k}, \vec{q}_1} F_1^{\downarrow,\downarrow}(\vec{k}, \vec{q}_1, -1; \omega) \right], \quad (\text{A2})$$

$$G_{\uparrow,\downarrow}(k, \omega) = G_0(k, \omega) \left[g \sum_{k, q_1} F_1^{\uparrow,\downarrow}(k, q_1, -1; \omega) \right], \quad (\text{A3})$$

$$G_{\downarrow,\uparrow}(\vec{k}, \omega) = G_0(\vec{k}, \omega) \left[g \sum_{\vec{k}, \vec{q}_1} F_1^{\downarrow,\uparrow}(\vec{k}, \vec{q}_1, +1; \omega) \right]. \quad (\text{A4})$$

As can be intuitively seen in Fig. 4, the nondiagonal element of the Green's function should be zero. To see this more systematically, one writes the one-boson Green's function as

$$\sum_{\vec{k}, \vec{q}_1} F_1^{\uparrow,\downarrow}(\vec{k}, \vec{q}_1, -1; \omega) = \frac{G_{\downarrow,\uparrow}(\vec{k}, \omega)}{gG_0(\vec{k}, \omega)}. \quad (\text{A5})$$

Repeating the equation of motion we obtain the two-boson amplitude

$$\begin{aligned} & \sum_{\vec{q}_1, \vec{q}_2} F_2^{\uparrow,\downarrow}(\vec{k}, \vec{q}_1, \vec{q}_2, -1, +1; \omega) \\ &= \frac{G_{\downarrow,\uparrow}(\vec{k}, \omega)}{gG_0(\vec{k}, \omega)} \left\{ \frac{1}{gG_0(\vec{k}, \omega)} - gG_0[\vec{k} - \vec{q}, \omega - \omega(\vec{q})] \right\}. \end{aligned} \quad (\text{A6})$$

Finally for order $N+1$, we obtain for even N ,

$$\begin{aligned} & \sum_{\vec{k}, \vec{q}_1, \vec{q}_2, \dots, \vec{q}_{N+1}} F_{N+1}^{\alpha, \alpha}(\vec{k}, \vec{q}_1, \vec{q}_2, \dots, +1, -1, \dots; \omega) \\ & = A(\vec{k}, \vec{q}_1, \vec{q}_2, \dots, +1, -1, \dots; \omega) G_{\uparrow, \downarrow}(\vec{k}, \omega) = 0, \end{aligned} \quad (\text{A7})$$

and for odd N ,

$$\begin{aligned} & \sum_{\vec{k}, \vec{q}_1, \vec{q}_2, \dots, \vec{q}_{N+1}} F_{N+1}^{\uparrow, \downarrow}(\vec{k}, \vec{q}_1, \vec{q}_2, \dots, +1, -1, \dots; \omega) \\ & = B(\vec{k}, \vec{q}_1, \vec{q}_2, \dots, +1, -1, \dots; \omega) G_{\uparrow, \downarrow}(\vec{k}, \omega) = 0. \end{aligned} \quad (\text{A8})$$

The A, B coefficients for various orders can be seen by inspection to be nonzero. This proves that the spin off-diagonal components of the Green's function are zero. This can be seen intuitively in Fig. 4.

To proceed further, we define a modified form of the bosonic Green's function in the MA(1) approximation as

$$\begin{aligned} & f_n^{\alpha, -\alpha}(\vec{k}, \vec{q}_1, \dots, \vec{q}_n, \dots, +1, -1, \dots; \omega) \\ & = \frac{g^n F_n^{\alpha, (-1)^n \alpha}(\vec{k}, \vec{q}_1, \dots, \vec{q}_n, \dots, +1, -1, \dots; \omega)}{G_{\alpha, \alpha}(\vec{k}, \omega)}. \end{aligned} \quad (\text{A9})$$

By inserting this in Eq. (4) one finds

$$G_{\alpha, \alpha}(\vec{k}, \omega) = ! G_0(\vec{k}, \omega) \left[1 + g \sum_{\vec{k}, \vec{q}_1} f_1^{\alpha, -\alpha}(\vec{k}, \vec{q}_1, 1; \omega) G_{\alpha, \alpha}(\vec{k}, \omega) \right], \quad (\text{A10})$$

where the matrix form of the Green's function is

$$G(k, \omega) = \begin{pmatrix} G_{\uparrow, \uparrow}(\vec{k}, \omega) & 0 \\ 0 & G_{\downarrow, \downarrow}(k, \omega) \end{pmatrix}. \quad (\text{A11})$$

Dyson's equation,

$$G_{\alpha, \alpha}(\vec{k}, \omega) = [\omega - \epsilon_{\vec{k}} - \Sigma^{\alpha, \alpha}(\vec{k}, \omega) + i\eta]^{-1}, \quad (\text{A12})$$

give the spin diagonal self-energy as

$$\Sigma^{\alpha, \alpha}(\omega) = \sum_{\vec{k}, \vec{q}_1} f_1^{\alpha, -\alpha}(\vec{k}, \vec{q}_1, +1; \omega). \quad (\text{A13})$$

So the MA(1) self-energy is diagonal and can be casted into the final form given by Eq. (8), where

$$A_1(\omega) = \frac{\bar{g}_{0,2}(\omega)}{1 - \frac{2\bar{g}_{0,3}(\omega)\bar{g}_{0,2}(\omega)}{1-\dots}},$$

$$A_2(\omega) = \frac{2\bar{g}_{0,2}(\omega)}{1 - \frac{3\bar{g}_{0,3}(\omega)\bar{g}_{0,2}(\omega)}{1-\dots}},$$

$$\bar{g}_{0,n}(\omega) = \sum_{\vec{k}, \vec{q}_1, \dots, \vec{q}_n} G_0\left(\vec{k} - \sum_i \vec{q}_i, \omega - \sum_i \omega_{\vec{q}_i}\right). \quad (\text{A14})$$

*sa.jafari@cc.iut.ac.ir

- ¹K. S. Novoselov, A. K. Geim, S. V. Morozov, D. Jiang, Y. Zhang, S. V. Dubonos, I. V. Grigorieva, and A. A. Firsov, *Science* **306**, 666 (2004); K. S. Novoselov, A. K. Geim, S. V. Morozov, D. Jiang, M. I. Katsnelson, I. V. Grigorieva, S. V. Dubonos, and A. A. Firsov, *Nature (London)* **438**, 197 (2005).
- ²For a review see: A. H. Castro Neto, F. Guinea, N. M. R. Peres, K. S. Novoselov, and A. K. Geim, *Rev. Mod. Phys.* **81**, 109 (2009).
- ³G. W. Semenoff, *Phys. Rev. Lett.* **53**, 2449 (1984).
- ⁴X. Du, I. Skachko, A. Barker, and E. Y. Andrei, *Nat. Nanotechnol.* **3**, 491 (2008).
- ⁵R. Saito, *Physical Properties of Carbon Nanotubes* (World Scientific, Singapore, 1998).
- ⁶I. A. Luk'yanchuk and Y. Kopelevich, *Phys. Rev. Lett.* **93**, 166402 (2004).
- ⁷S. Y. Zhou, G.-H. Gweon, J. Graf, A. V. Fedorov, C. D. Spataru, R. D. Diehl, Y. Kopelevich, D.-H. Lee, S. G. Louie, and A. Lanzara, *Nat. Phys.* **2**, 595 (2006).
- ⁸G. Baskaran and S. A. Jafari, *Phys. Rev. Lett.* **89**, 016402 (2002).
- ⁹S. A. Jafari and G. Baskaran, *Eur. Phys. J. B* **43**, 175 (2005).
- ¹⁰G. Moos, C. Gahl, R. Fasel, M. Wolf, and T. Hertel, *Phys. Rev. Lett.* **87**, 267402 (2001).
- ¹¹C. D. Spataru, M. A. Cazalilla, A. Rubio, L. X. Benedict, P. M. Echenique, and S. G. Louie, *Phys. Rev. Lett.* **87**, 246405 (2001).
- ¹²A. Bostwick, T. Ohta, T. Seyller, K. Horn, and E. Rotenberg, *Nat. Phys.* **3**, 36 (2007).

- ¹³E. H. Hwang, Ben Yu-Kuang Hu, and S. Das Sarma, *Phys. Rev. B* **76**, 115434 (2007).
- ¹⁴E. H. Hwang and S. Das Sarma, *Phys. Rev. B* **75**, 205418 (2007).
- ¹⁵J. Gonzalez, F. Guinea, and M. A. H. Vozmediano, *Phys. Rev. Lett.* **77**, 3589 (1996); *Phys. Rev. B* **63**, 134421 (2001).
- ¹⁶G. Li, A. Luican, and E. Y. Andrei, arXiv:0803.4016 (unpublished); J. L. McChesney, A. Bostwick, T. Ohta, K. Emtsev, T. Seyller, K. Horn, and E. Rotenberg, arXiv:0809.4046 (unpublished).
- ¹⁷D. V. Khveshchenko, *Phys. Rev. Lett.* **87**, 206401 (2001).
- ¹⁸Y. Kopelevich, *Braz. J. Phys.* **33**, 737 (2003); Y. Kopelevich, J. C. Medina Pantoja, R. R. da Silva, and S. Moehlecke, *Phys. Rev. B* **73**, 165128 (2006).
- ¹⁹J. G. Checkelsky, Lu Li, and N. P. Ong, *Phys. Rev. Lett.* **100**, 206801 (2008); *Phys. Rev. B* **79**, 115434 (2009).
- ²⁰M. Berciu, *Phys. Rev. Lett.* **97**, 036402 (2006).
- ²¹G. Baskaran and E. Tosatti, *Curr. Sci.* **61**, 33 (1991).
- ²²S. Pathak, V. B. Shenoy, and G. Baskaran, arXiv:0809.0244 (unpublished).
- ²³Glen L. Goodvin, Mona Berciu, and George A. Sawatzky, *Phys. Rev. B* **74**, 245104 (2006); M. Berciu and G. L. Goodvin, *ibid.* **76**, 165109 (2007).
- ²⁴L. Covaci and M. Berciu, *Phys. Rev. Lett.* **100**, 256405 (2008).
- ²⁵G. D. Mahan, *Many Particle Physics* (Plenum, New York, 1981).
- ²⁶J. Gonzalez and E. Perfetto, *Phys. Rev. Lett.* **101**, 176802 (2008); Cheol-Hwan Park, F. Giustino, Marvin L. Cohen, and S. G. Louie, *ibid.* **99**, 086804 (2007).